Adaptive Inverse Compensation Fault-Tolerant Control for a Flexible Manipulator With Unknown Dead-Zone and Actuator Faults

Zhijia Zhao, *Member, IEEE*, Zhifeng Tan, Zhijie Liu, *Member, IEEE*, Mehmet Onder Efe, *Senior Member, IEEE*, and Choon Ki Ahn, *Senior Member, IEEE*

***Abstract*—This study presents an adaptive inverse compensation control of a flexible single-link manipulator with an unknown dead-zone and actuator faults. First, a dead-zone inverse model and a smooth inverse operator are constructed to address dead-zone nonlinearity. Second, an adaptive fault-tolerant control is utilized to compensate for the partial loss of the effectiveness of the actuator. Third, the coupling errors of the dead-zone and faults are effectively removed and resolved by introducing an estimate for unknown bounds. Then, the direct Lyapunov theory is used to guarantee uniformly ultimately bounded stability in the controlled system. Finally, the simulations and experiments demonstrate the efficiency of the presented method.**

***Index Terms*—Adaptive control, fault-tolerant control (FTC), flexible manipulator, inverse compensation, vibration control.**

Manuscript received 9 August 2022; revised 4 November 2022 and 10 December 2022; accepted 10 January 2023. Date of publication 31 January 2023; date of current version 9 June 2023. This work was supported in part by the National Natural Science Foundation of China under Grant 62273112, Grant 62103039, and Grant 62073030, in part by the Scientific Research Projects of Guangzhou Education Bureau under Grant 202032793, in part by the Science and Technology Planning Project of Guangzhou City under Grant 202102010398 and Grant 202201010758, in part by the Guangzhou University-Hong Kong University of Science and Technology Joint Research Collaboration Fund under Grant YH202205, in part by the Open Research Fund from the Guangdong Laboratory of Artificial Intelligence and Digital Economy [Shenzhen (SZ)] under Grant GML-KF-22-27, in part by the Scientific and Technological Innovation Foundation of Shunde Graduate School, University of Science and Technology Beijing (USTB) under Grant BK21BF003, in part by the Beijing Top Discipline for Artificial Intelligent Science and Engineering, USTB, and in part by the National Research Foundation of Korea (NRF) grant funded by the Korea government (Ministry of Science and ICT) under Grant NRF-2020R1A2C1005449. *(Corresponding authors: Zhijie Liu; Choon Ki Ahn.)*

Zhijia Zhao and Zhifeng Tan are with the School of Mechanical and Electrical Engineering, Guangzhou University, Guangzhou, Guangdong 510006, China, and also with the Guangdong Laboratory of Artificial Intelligence and Digital Economy (SZ), Shenzhen 518060, China (e-mail: zhaozj@gzhu.edu.cn; 2112107119@e.gzhu.edu.cn).

Zhijie Liu is with the School of Intelligence Science and Technology, University of Science and Technology Beijing, Beijing 100083, China (e-mail: liuzhijie@ustb.edu.cn).

Mehmet Onder Efe is with the Department of Computer Engineering, Hacettepe University, 06800 Ankara, Turkey (e-mail: onderefe@hacettepe.edu.tr).

Choon Ki Ahn is with the School of Electrical Engineering, Korea University, Seoul 136-701, South Korea (e-mail: hironaka@korea.ac.kr).

Color versions of one or more figures in this article are available at https://doi.org/10.1109/TIE.2023.3239926.

Digital Object Identifier 10.1109/TIE.2023.3239926

I. Introduction

With the development of technology, robot manipulators have been broadly applied to agriculture, industry, medicine, national defense, and other fields [1]. In comparison to rigid manipulators [2], the flexible manipulators have a broader application characterized by their light weight, lower energy wastage, and fast speed, and they have garnered significant attention over the past few years [3]. Nevertheless, the flexibility of the structure may cause oscillation and deformation during the task, which may affect the control precision and shorten the service life. Thus, developing efficient vibration elimination schemes is important.

Owing to nonintrusive sensing and actuation, boundary control (BC) is an applicable and practical method for stabilizing flexible manipulators [4], [5]. Recently, significant advances have been achieved in the BC of flexible manipulators [6], [7], [8], [9], [10]. In [6], a BC mounted on a hub was established to guarantee that the system states converged exponentially to a stable position under ideal conditions. In [7], considering input backlash, a BC was designed to track the target angle and eliminate vibrations. A boundary output feedback control was presented for an input-saturated flexible manipulator, and a set of observers was introduced to observe the immeasurable system states in [8]. In [9], for an externally disturbed flexible manipulator, a BC was established at the tip of the link to restrain elastic vibration, and the torque input regulated the joint position. An adaptive neural network (NN) BC was proposed in [10] to address modeling uncertainties and input constraints in flexible manipulators.

Dead-zone nonlinearity is ubiquitous in actuators of physical control systems, such as motors, valves, and hydraulic components, with the characteristic that the system does not respond to a given input until it reaches a specific level. Ignoring the dead-zone may contribute to unacceptable performance during controller design. In recent years, numerous approaches

0278-0046 © 2023 IEEE. Personal use is permitted, but republication/redistribution requires IEEE permission.
See https://www.ieee.org/publications/rights/index.html for more information.

Authorized licensed use limited to: ULAKBIM UASL - Hacettepe Universitesi. Downloaded on August 30,2023 at 13:44:49 UTC from IEEE Xplore. Restrictions apply.

have been proposed to eliminate dead-zone effects. In [11], an NN control was established to eliminate the dead-zone effects. Owing to its strong robustness and anti-interference ability, sliding-mode control was exploited to address dead zones in [12]. In [13], dead-zone was perceived as a bounded extrinsic disturbance, and adaptive fuzzy controllers were developed to cope with it. In addition, adaptive inverse compensation is considered another effective method for handling dead-zone nonlinearity [14], [15]. In [16], a smooth dead-zone inverse projection was presented to avoid chattering. Moreover, a novel backstepping compensation control was constructed for accommodating uncertain dead-zone in nonlinear systems [17]. In [18], a new composite adaptive control was established for a dynamically positioning vehicle by constructing inverse compensating terms, and the constraints from dead-zone nonlinearity could be effectively released. Despite the adaptive inverse control for finite-dimensional systems with dead-zone nonlinearity having been successfully attained in the aforementioned studies, there are no results available concerning the inverse compensation control for infinite-dimensional flexible manipulator systems constrained by dead-zone nonlinearity; this presents the motivation for our research.

In practice, actuator faults universally occur when operating in control mechanisms, which generally affect the control performance of the plant and may cause accidents. Over the past decade, several mature control strategies have been established to ensure acceptable and stable performance of systems with actuator faults, such as learning control [19], observer-based control [20], [21], and sliding-mode control [22], [23]. In addition, adaptive fault-tolerant control (FTC) (AFTC) has been broadly utilized to compensate for unknown failures or faults in nonlinear systems, owing to its strong ability to compensate and robustness of faults [24], [25], [26]. Meanwhile, the AFTC for flexible manipulators has achieved tremendous progress. In [27], an AFTC was put forward for flexible-rigid manipulators with state constraints. In [28], a flexible manipulator, including piezoelectric controllers installed at the flexible link and a direct current (DC) motor at the joint, was investigated, and an adaptive compensation method was employed to accommodate an infinite number of actuator failures. An AFTC strategy was established for flexible manipulators with actuator faults in an infinite number [29]. To the best of authors' knowledge, despite the significant advances having been achieved in AFTC for flexible manipulator systems, there is a paucity of research on AFTC to compensate for the hybrid effects of unknown dead-zone nonlinearity and actuator faults in flexible manipulator systems, thus inspiring us to conduct further exploration.

Motivated by the described analysis and summary, we aim to investigate the control problem for a flexible manipulator with dead-zone nonlinearity and actuator faults. The main contributions of this study are as follows.

1) Compared with the present flexible structure control [10], [30] that considered the input nonlinearity as an external bounded disturbance, we introduce smooth dead-zone inverse dynamics to better tackle the dead-zone nonlinearity in a flexible manipulator system; then, the dead-zone characteristic is reformulated in the form of an expected control signal and a small bounded error through derivation.
2) Different from the work in [29], an adaptive fault compensation factor without projection is used in this study. In contrast with [18], [28], which used robust adaptive compensation to dispose of the effects of actuator faults or unknown dead-zone, a smoother adaptive compensation updating law of unknown bounds is developed to address the resulting coupling of the bias faults and dead-zone, which avoids complexity and achieves a good performance.
3) The direct Lyapunov method is adopted to guarantee the controlled system stability, and numerical simulations with the comparison of other methods validate the control performance. Furthermore, an experimental investigation based on the Quanser flexible link system proves the practicability and efficacy of the proposed scheme.

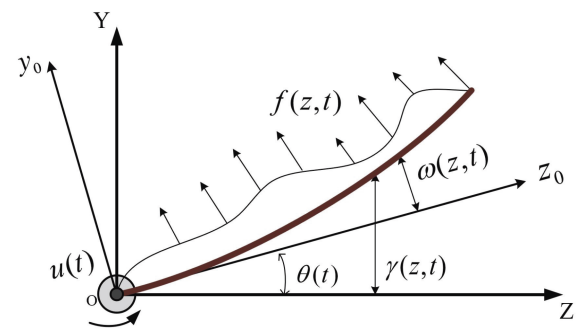

Fig. 1. Structural diagram of the flexible manipulator.

Notation: Hereinafter, $\mathcal{R}$ and $\mathcal{R}^+$ denote the sets of real numbers and positive real numbers, respectively. $\Re^{a\times b}$ represents the sets of all real $a \times b$ matrices. A positive symmetric matrix expresses as $E \succ 0$. $\lambda_{\max}(E)$ stands for the maximum eigenvalues of the matrix. To simplify the expression, some symbols are defined as follows: $(\circ) = (\circ)(z,t)$, $(\circ)' = \partial(\circ)/\partial z$, $(\dot{\circ}) = \partial(\circ)/\partial t$, $(\circ)'' = \partial^2(\circ)/\partial z^2$, $(\ddot{\circ}) = \partial^2(\circ)/\partial t^2$, $(\circ)''' = \partial^3(\circ)/\partial z^3$, $(\circ)'''' = \partial^4(\circ)/\partial z^4$, $(\circ)_0 = \circ(0,t)$, $(\circ)_l = \circ(l,t)$, and $\tilde{\circ} = \circ - \hat{\circ}$.

II. Problem Statement and Preliminaries

A. Dynamic Model of the Flexible Manipulator

The geometry of flexible manipulator systems is depicted in Fig. 1, in which the coordinate axes ZOY and z_0oy_0 represent the global and local rotating inertial coordinate systems, respectively. t and z denote the independent time and space variables, respectively. The length of the link is l, $\omega(z,t)$ denotes the elastic deflection in the rotating inertial coordinate system, $f(z,t)$ is the external disturbance, $\theta(t)$ denotes the angle, $u(t)$ represents the actuator input, and $\gamma(z,t) = z\theta(t) + \omega(z,t)$ denotes the total displacement of the link in the coordinate axis ZOY.

Authorized licensed use limited to: ULAKBIM UASL - Hacettepe Universitesi. Downloaded on August 30,2023 at 13:44:49 UTC from IEEE Xplore. Restrictions apply.

First, the system's dynamical model is presented as follows [7]:

$$\rho\ddot{\gamma}(z,t)+c\dot{\gamma}(z,t)=-EI\omega''''(z,t)+T\omega''(z,t)+f(z,t)$$
$$\forall(z,t)\in(0,l)\times[0,+\infty) \tag{1}$$
$$EI\omega'''(l,t)=T\omega'(l,t) \tag{2}$$
$$\omega(0,t)=\omega'(0,t)=\omega''(l,t)=0 \tag{3}$$

and the angle position dynamics are formulated as

$$I\ddot{\theta}(t)=EI\omega''(0,t)+T\omega(l,t)+u(t),\quad t\in[0,+\infty) \tag{4}$$

where EI, c, T, and ρ describe the bending stiffness, viscosity coefficient, tension, and density, respectively.

B. Actuator Faults and Dead-Zone Nonlinearity Analysis

According to [31], the actuator fault expression is described as

$$u(t)=\sigma u_f(t)+u_s(t) \tag{5}$$

where $\sigma\in(0,1]$ denotes an unknown effectiveness coefficient and $u_s(t)$ represents an unknown function representing the bias fault. Notably, the total loss of effectiveness is not considered because only one actuator is in the system.

Remark 1: Several prior studies have extended the different classes of FTC. For example, 1) Fault accommodation [32]: The system can keep good performance by adjusting controller parameters to adapt the parameters of the faulty plant. 2) Control reconfiguration [32]: The corresponding redundant components are needed to keep the system running when the accommodation cannot be used similarly to the actuator breakdown. In this study, we employ fault accommodation to handle the fault in the actuator.

As aforementioned, the dead-zone is universal in dc motors and the characteristic $DZ(\bullet)$ can be expressed as follows [33]:

$$u_f(t)=DZ(\varpi(t))=\begin{cases} m_r(\varpi(t)-k_r), & \text{if } \varpi(t)\geq k_r\\ 0, & \text{if } k_r<\varpi(t)<k_l\\ m_l(\varpi(t)-k_l), & \text{if } \varpi(t)\leq k_l\end{cases} \tag{6}$$

where $m_r>0$ and $m_l>0$ denote the slopes of the lines with $|m_r|\neq|m_l|$, $k_r>0$, and $k_l<0$ are the break-points with $|k_r|\neq|k_l|$. $\varpi(t)$ describes a desired actuator input to be designed, and $u_f(t)$ denotes an actual actuator output influenced by dead-zone. Then, a dead-zone inverse dynamics model is introduced as follows:

$$\varpi(t)=\frac{u_f+m_rk_r}{m_r}\Phi_r(u_f)+\frac{u_f+m_lk_l}{m_l}\Phi_l(u_f) \tag{7}$$

where smooth functions $\Phi_r(u_f)$ and $\Phi_l(u_f)$ are defined as

$$\Phi_r(u_f)=\frac{1+\tanh(\tau u_f)}{2},\quad \Phi_l(u_f)=\frac{1-\tanh(\tau u_f)}{2} \tag{8}$$

with τ being a positive constant.

To facilitate this illustration, we parameterize the dead-zone model (6) as

$$u_f(t)=\psi^T\nu \tag{9}$$

where

$$\psi=[m_r,m_rk_r,m_l,m_lk_l]^T \tag{10}$$
$$\nu=[\mu_r(t)\varpi(t),-\mu_r(t),\mu_l(t)\varpi(t),-\mu_l(t)]^T \tag{11}$$
$$\mu_r=\begin{cases}1, & \text{if } u_f(t)>0\\ 0, & \text{otherwise,}\end{cases}\qquad \mu_l=\begin{cases}1, & \text{if } u_f(t)<0\\ 0, & \text{otherwise.}\end{cases} \tag{12}$$

Notably, the parameters m_r, m_l, k_r, and k_l in (10) are unknown and ν in (11) is unavailable in practice. To address the dead-zone parameter uncertainties, the expected actuator input in (7) can be expressed as

$$\varpi(t)=\frac{u_r+\widehat{m_rk_r}}{\widehat{m}_r}\Phi_r(u_r)+\frac{u_r+\widehat{m_lk_l}}{\widehat{m}_l}\Phi_l(u_r) \tag{13}$$

where the actual control input u_r is designed in Section III. Besides, $\hat{\psi}$ is an estimation of ψ, and $\hat{\psi}$ and $\hat{\nu}$ are defined as

$$\hat{\psi}=[\widehat{m}_r,\widehat{m_rk_r},\widehat{m}_l,\widehat{m_lk_l}]^T \tag{14}$$
$$\hat{\nu}=[\Phi_r(\varpi)\varpi(t),-\Phi_r(\varpi),\Phi_l(\varpi)\varpi(t),-\Phi_l(\varpi)]^T. \tag{15}$$

Hence, according to (13)–(15), the actual control input is rewritten as

$$u_r(t)=\hat{\psi}^T\hat{\nu}. \tag{16}$$

Moreover, invoking (9) and (16), we formulate the compensation error as

$$u_f(t)-u_r(t)=(\psi-\hat{\psi})^T\hat{\nu}(t)+d_e(t) \tag{17}$$

where $d_e(t)=\psi^T(\hat{\nu}-\nu)$, and by invoking [16], we determine that $|d_e(t)|$ is upper bound, which can be obtained as

$$|d_e(t)|\leq\begin{cases}\frac{1}{2}e^{-1}|m_r-m_l|/\tau+\frac{|m_rk_r-m_lk_l|}{e^{2k_r\tau}+1}, & \text{if } \varpi(t)\geq k_r\\ \frac{1}{2}e^{-1}|m_r-m_l|/\tau+\frac{|m_rk_r-m_lk_l|}{e^{-2k_l\tau}+1}, & \text{if } \varpi(t)\leq k_l\\ \max\{m_r,m_l\}|k_r-k_l|, & \text{otherwise.}\end{cases} \tag{18}$$

Remark 2: When $k_l<\varpi(t)<k_r$, $d_e(t)$ is bounded. When ϖ exceeds this range (k_l,k_r), the bound on $d_e(t)$ decreases as τ increases. Thus, $d_e(t)$ is bounded when $t\geq 0$ and $d_e(t)$ approaches zero as $\tau\to+\infty$.

Thus, by combining (5) and (17), the actual fault model is expressed as

$$u(t)=\sigma u_r(t)+\sigma\tilde{\psi}^T\hat{\nu}+\sigma d_e(t)+u_s(t). \tag{19}$$

C. Preliminaries

This section presents the following assumptions, remarks, and lemmas for promoting follow-up analysis.

Assumption 1 [34]: There exists a constant $\bar{f}\in\mathcal{R}^+$ satisfying $|f(z,t)|\leq\bar{f}$, $\forall(z,t)\in(0,l)\times(0,+\infty)$. Because the energy of the disturbance $f(z,t)$ is finite, this assumption is considered reasonable.

Assumption 2 [18]: For the dead-zone parameters m_r and m_l, positive constants $\underline{m_r}$ and $\underline{m_l}$ satisfy $m_r\geq\underline{m_r}>0$ and $m_l\geq\underline{m_l}>0$. For the bias fault, there exists a positive constant $\bar{u}_s$ satisfying $|u_s|\leq\bar{u}_s$.

Remark 3: From the point of view of mathematics, the flexible manipulator is a distributed parameter system (DPS) with

Authorized licensed use limited to: ULAKBIM UASL - Hacettepe Universitesi. Downloaded on August 30,2023 at 13:44:49 UTC from IEEE Xplore. Restrictions apply.

infinite-dimensional state spaces, and the motion of the system is described by variables depending on both time and space. DPSs are generally affected by distributed disturbances. It means that the DPS may suffer varying degrees of external effects in distinct times and spaces. $f(z,t)$ in Assumption 1 is the distributed disturbance on the flexible manipulator, which is related to the variables of time t and space z, and is caused by the effects of the gust of wind in complex environments.

Lemmas 1–3 are provided in Appendix A.

III. Control Design

This article proposes the design of an adaptive inverse compensation FTC to compensate for the effects of unknown dead-zone and actuator faults such that the elastic deflection $\omega(z,t)$ is suppressed and the tracking error is uniformly ultimately bounded.

A. Control Design

The actual control input is proposed as follows:

$$u_r(t) = -\hat{p}u_d \tag{20}$$

where $\hat{p}$ represents an estimate of p with $p = \frac{1}{\sigma}$, and u_d is given as

$$u_d(t) = b_1\alpha + (b_2+T)\omega_l + \beta I\dot{\theta}(t) + b_\theta[\theta(t)-\theta_r] + \frac{\alpha\hat{\Theta}^2}{\sqrt{\alpha^2\hat{\Theta}^2+\zeta^2(t)}} \tag{21}$$

where b_1, b_2, η, $b_\theta > 0$, α is defined as $\alpha = \dot{\theta} + \eta[\theta(t)-\theta_r]$, $\zeta(t)$ is a positive and monotone decreasing function, and $\hat{\Theta}$ denotes the estimation of the upper bound Θ defined as $\Theta = \sup|\sigma d_e(t) + u_s(t)|, t \in [0,+\infty)$. At this moment, we construct the adaptive updating laws as

$$\dot{\hat{\psi}} = \text{Proj}\{\delta\alpha\hat{\nu}\} \tag{22}$$

$$\dot{\hat{\Theta}} = \alpha - \varrho_1\hat{\Theta} \tag{23}$$

$$\dot{\hat{p}} = \alpha\gamma_a u_d - \varrho_2\hat{p} \tag{24}$$

where ϱ_1, ϱ_2, and γ_a are positive constants, $\delta \in \Re^{4\times4} \succ 0$. Proj$\{\bullet\}$ is the projection mapping operator described in [35]

$$\text{Proj}\{\bullet\} = \begin{cases} \bullet, & \text{if } \hat{\psi} \in \mathring{\Pi} \\ \text{or} \quad \nabla_{\hat{\psi}}\mathcal{P}^T\bullet \le 0 & \\ \left(\bullet - \Gamma\frac{\nabla_{\hat{\psi}}\mathcal{P}\nabla_{\hat{\psi}}\mathcal{P}^T}{\nabla_{\hat{\psi}}\mathcal{P}^T\Gamma\nabla_{\hat{\psi}}\mathcal{P}}\bullet\right), & \text{if } \hat{\psi} \in \bar{\Pi} \\ \text{and} \quad \nabla_{\hat{\psi}}\mathcal{P}^T\bullet > 0 & \end{cases} \tag{25}$$

where $\mathring{\Pi}$ and $\bar{\Pi}$ denote the interior and the boundary of the set $\Pi \in \Re$, respectively. $\nabla_{\hat{\psi}}\mathcal{P}$ represents an outward normal vector at $\bar{\Pi}$. Proj$\{\bullet\}$ is used to ensure that the value of $\hat{\psi}$ is restricted within a certain range, $\Gamma \succ 0$.

Remark 4: Fig. 2 depicts the chart of the controlled system. The signals $\theta(t)$ and ω_l are available directly by the encoder and strain gauge. Moreover, the angle velocity $\dot{\theta}(t)$ is calculated employing the measured $\theta(t)$.

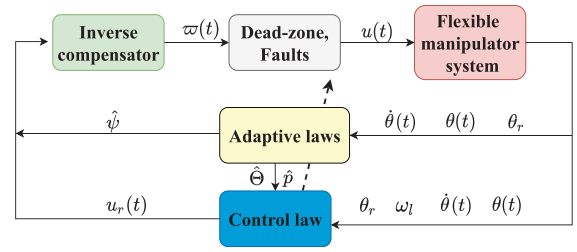

Fig. 2. Diagram of the controlled system.

B. Stability Analysis

Now, the Lyapunov function candidate is defined as

$$V_a(t) = V_{a1}(t) + V_{a2}(t) + V_{a3}(t) + V_{a4}(t) \tag{26}$$

where

$$V_{a1}(t) = \frac{1}{2}\rho\int_0^l \dot{\gamma}^2 dz + \frac{1}{2}EI\int_0^l \omega''^2 dz + \frac{1}{2}T\int_0^l \omega'^2 dz \tag{27}$$

$$V_{a2}(t) = \frac{1}{2}I\alpha^2 + \frac{1}{2}b_\theta[\theta(t)-\theta_r]^2 \tag{28}$$

$$V_{a3}(t) = \eta\rho\int_0^l \dot{\gamma}(z,t)\gamma_d(z,t)dz \tag{29}$$

$$V_{a4}(t) = \frac{\sigma}{2}\tilde{\psi}^T\delta^{-1}\tilde{\psi} + \frac{\sigma}{2\gamma_a}\tilde{p}^2 + \frac{1}{2}\tilde{\Theta}^2 \tag{30}$$

where $\gamma_d(z,t) = \omega + z[\theta-\theta_r]$ and $\dot{\gamma}(z,t) = \dot{\gamma}_d(z,t)$.

Lemma 4: The Lyapunov function (26) has upper and lower boundaries as follows:

$$0 \le \Lambda_1[V(t) + V_{a4}(t)] \le V_a(t) \le \Lambda_2[V(t) + V_{a4}(t)] \tag{31}$$

with Λ_1 and Λ_2 being positive constants.

Proof: Refer to Appendix B.

Lemma 5: The differentiation of (26) has the following upper bound:

$$\dot{V}_a(t) \le -\Lambda V_a(t) + \epsilon \tag{32}$$

where Λ, $\epsilon > 0$.

Proof: Refer to Appendix C.

Theorem 1: For flexible manipulator systems affected by dead-zone and actuator faults, under the established control (20) and (21), the adaptive updating laws (22)–(24), and bounded initial conditions, by properly selecting the designed parameters to satisfy constraints (52)–(55), we conclude that the system states are bounded and converge to a small neighborhood of origin.

Proof: Multiplying (32) by $e^{\Lambda t}$ yields

$$\frac{\partial}{\partial t}[V_a(t)e^{\Lambda t}] \le \epsilon e^{\Lambda t}. \tag{33}$$

Authorized licensed use limited to: ULAKBIM UASL - Hacettepe Universitesi. Downloaded on August 30,2023 at 13:44:49 UTC from IEEE Xplore. Restrictions apply.

Integrating (33) gives

$$V_a(t) \leq \left[V_a(0) - \frac{\epsilon}{\Lambda}\right] e^{-\Lambda t} + \frac{\epsilon}{\Lambda}. \tag{34}$$

Using Lemma 2 and (27) yields

$$\frac{1}{2l}\eta T\omega^2 \leq \frac{\eta}{2}T\int_0^l \omega'^2 dz \leq V_{a1}(t) \leq \frac{1}{\Lambda_1}V_a(t). \tag{35}$$

Substituting (35) into (34) results in

$$|\omega(z,t)| \leq \sqrt{\frac{2l}{\eta T\Lambda_1}\left[V_a(0) + \frac{\epsilon}{\Lambda}\right]}, \forall (z,t) \in [0,l] \times [0,+\infty). \tag{36}$$

Furthermore, we have

$$\lim_{t\to+\infty} |\omega(z,t)| \leq \sqrt{\frac{2l\epsilon}{\eta T\Lambda_1\Lambda}} \quad \forall z \in [0,l]. \tag{37}$$

Similarly, from (28), we have

$$|\theta(t) - \theta_r| \leq \sqrt{\frac{2l}{b_\theta\Lambda_1}\left[V_a(0) + \frac{\epsilon}{\Lambda}\right]} \quad \forall t \in [0,+\infty). \tag{38}$$

Then, we arrive at

$$\lim_{t\to+\infty} |\theta(t) - \theta_r| \leq \sqrt{\frac{2l\epsilon}{b_\theta\Lambda_1\Lambda}}. \tag{39}$$

Remark 5: The parameter settings must satisfy Lemma 4 and constraint conditions (52)–(55). The following selection process for parameters is provided. First, an appropriate parameter η is chosen to guarantee Lemma 4. Next, selecting suitable parameters ϕ_1, ϕ_2, ϕ_3, b_2, and b_1 makes (52), (53), and (55) hold. Then, we determine proper ϕ_4 and b_θ to satisfy (54). Moreover, according to (57), we can infer that the convergence speed gets faster and the convergence region becomes smaller as b_θ, b_2, ϱ_1, and ϱ_2 increase and b_1 decreases. During the parameter adjusting, appropriate values of η, b_θ, b_2, ϱ_1, b_1, and ϱ_2 are suitably tuned until excellent transient and steady-state performance is acquired. Above can provide a reference to the design parameter selection for adjusting the control performance.

Remark 6: In this study, our main concern lies in addressing the unknown dead-zone and actuator faults in the flexible manipulator system. The parameter adjusting method stated in Remark 5 is mainly based on the individual experience due to the ease of execution, and how to establish systematic approaches for the most appropriately selecting design parameters remains an open issue and will be a future research direction.

IV. Numerical Simulation

We demonstrate the efficacy of the presented dead-zone inverse FTC (DIFTC) on MATLAB using the finite difference method and the system parameters are listed in Table I. The initial states of the flexible manipulator are set as $\theta(0) = 0$ rad, $\omega(z,0) = 0.5z^2$ m, $\dot{\theta}(0) = 0$ rad/s, and $\dot{\omega}(z,0) = 0$ m/s. The reference signal θ_r is set to $\theta_r = \frac{\pi}{6}$ rad. The parameters selected for the DIFTC are $b = 0.28$, $b_1 = 0.01$, $\eta = 0.05$, $b_\theta = 4.5$, and $\zeta(t) = 0.3e^{-0.1t}$. The parameters of the adaptive laws are selected as $\hat{\psi}(0) = [1.1, 0.22, 1.2, -0.23]^T$, $\hat{\Theta}(0) = 0.3$, $\gamma = 5$, $\varrho_1 = 0.1$, and $\varrho_2 = 5$. The set Π is given as $\Pi := \{\hat{\psi} \in \Re^{4\times 1} | 0.8 \leq \hat{m}_r \leq 1.2, 0.17 \leq \widehat{m_r k_r} \leq 0.23, 0.8 \leq m_l \leq 1.2, -0.25 \leq \widehat{m_l k_l} \leq -0.18\}$. The fault and dead-zone parameters are $\sigma = 0.3$, $u_s(t) = 0.05e^{-0.1t}$, $m_r = 1$, $m_l = 1.1$, $k_r = 0.2$, and $k_l = -0.2$, respectively. The actuator $u(t)$ suffers faults at 0.5 s.

TABLE I
System Parameters

Parameter	Value	Parameter	Value
EI	0.157 Nm^2	l	0.419 m
c	0.04NS/m	ρ	0.1 kg/m
I	0.0038 kgm^2	T	0.1 N

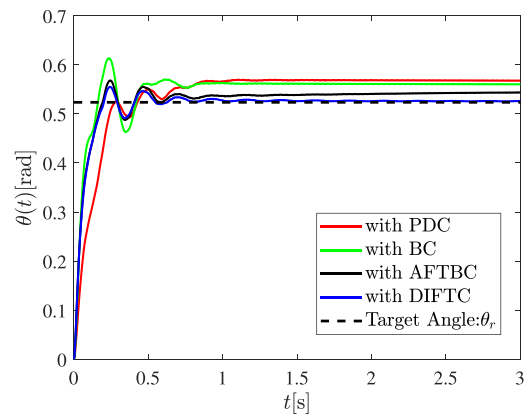

Fig. 3. Angular trajectory with different control methods.

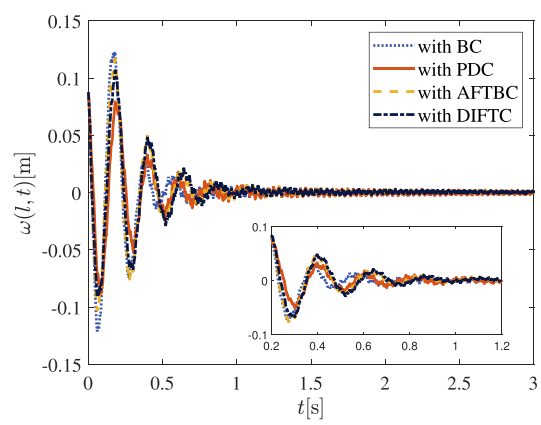

Fig. 4. Boundary deformation with different control methods.

To further verify the control performance, the BC [6], proportion differentiation control (PDC), and adaptive fault-tolerant BC (AFTBC) [30], are compared with the DIFTC, and Figs. 3–5 depicts simulation results. Table II gives the performance index of different methods based on the integral square error (ISE), integral time square error (ITSE), and integral time absolute error (ITAE).

Remark 7: The BC method in [6] does not consider the dead-zone and actuator faults. The PDC method is similar to a model-free approach based on the error and its derivative. The AFTBC regards the dead-zone as an external bounded

Authorized licensed use limited to: ULAKBIM UASL - Hacettepe Universitesi. Downloaded on August 30,2023 at 13:44:49 UTC from IEEE Xplore. Restrictions apply.

TABLE II
COMPARISON OF DIFFERENT APPROACHES IN SIMULATION, ISE, ITSE, ITAE AS PERFORMANCE INDEX

Index	Tracking Performance					Tip Deflection			
	Methods	PDC	BC	AFTBC	DIFTC	PDC	BC	AFTBC	DIFTC
ISE	-	583.59	348.88	269.50	253.67	26.16	51.50	47.03	50.11
ITSE	-	0.6657	0.0392	0.0303	0.0285	0.0029	0.0058	0.0053	0.0056
ITAE	-	0.4926	0.4104	0.2367	0.1642	0.0697	0.0851	0.0923	0.0969

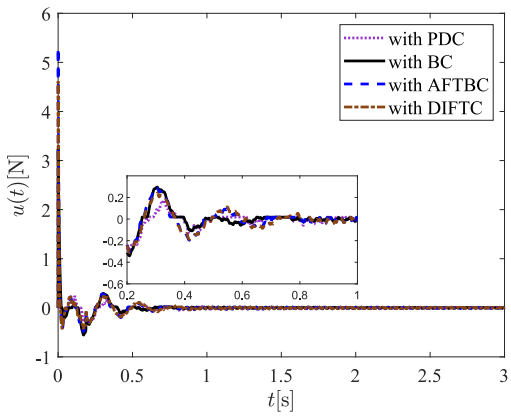

Fig. 5. Control signal with different control methods.

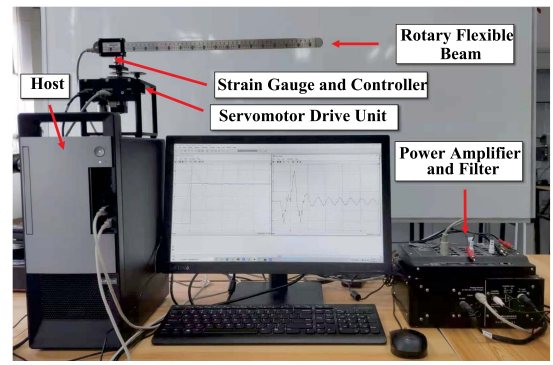

Fig. 6. Rotary flexible link system.

disturbance that is addressed by employing the robust adaptive method. The proposed strategy adopts the inverse operator and adaptive coefficient compensation to resolve unknown dead-zone and actuator faults.

The angle tracking and boundary deformation damping for the flexible manipulator with dead-zone and actuator faults are displayed in Figs. 3 and 4. As illustrated in Fig. 3, with the BC strategy, there is a slightly larger overshoot, and the steady-state tracking error is unacceptable under the PDC and BC, resulting in unsatisfactory performance. There is a lesser overshoot with AFTBC; however, the tracking error is not very satisfying. In contrast, with the DIFTC, the angular position can asymptotically track the desired trajectory. Meanwhile, it can be observed that under these methods, the deformation can converge around zero within 1 s. Under the BC and PDC, the deformation converges at a relatively fast speed. The suppression performance of boundary deformation with AFTBC and DIFTC is seen to be basically consistent. Note that, although the deformation is convergent under BC, PDC, and AFTBC, the angular position tracking performance is unsatisfactory. The control inputs are described in Fig. 5, and it is evident that the dead-zone nonlinearity is sufficiently compensated. The performance index table verifies the abovementioned analysis.

On the basis of the abovementioned results, we conclude that even if the system is affected by actuator faults and an unknown dead-zone, the suggested control can still maintain the excellent performance of the angular tracking and vibration suppression.

V. EXPERIMENT

To further validate the control performance, physical experiments are conducted on the Quanser experimental platform, as displayed in Fig. 6. The comparison is similar to the simulation.

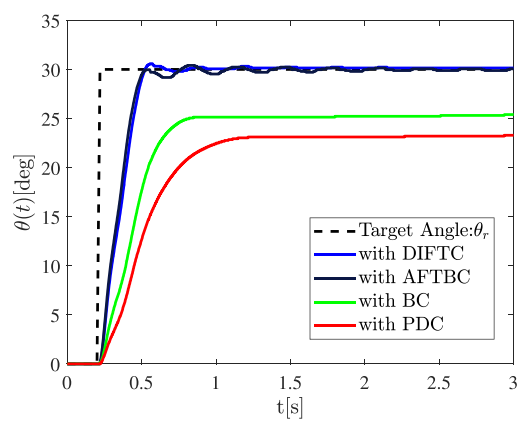

Fig. 7. Angular trajectory with different control methods under 30% partial loss of effectiveness.

TABLE III
COMPARISON OF DIFFERENT APPROACHES IN SIMULATION, ISE, ITSE, ITAE AS PERFORMANCE INDEX

Eff	Index	Tracking Performance				
		Methods	PDC	BC	AFTBC	DIFTC
30%	ISE	-	166310	106110	41857	38016
	ITSE	-	997.85	636.65	251.14	228.09
	ITAE	-	78.82	57.38	14.12	13.17
50%	ISE	-	109840	59812	31626	28487
	ITSE	-	659.07	358.87	189.75	170.92
	ITAE	-	61.73	33.66	11.69	11.17
70%	ISE	-	69308	35708	31626	24925
	ITSE	-	415.85	214.25	165.80	149.55
	ITAE	-	41.57	15.97	10.65	10.50

In addition, we consider different partial losses of effectiveness. Under 30%, 50%, and 70% partial loss of effectiveness of the actuator, the responses of the angular position are depicted in Figs. 7–9. Table III gives the performance index of different methods based on the ISE, ITSE, and ITAE.

Authorized licensed use limited to: ULAKBIM UASL - Hacettepe Universitesi. Downloaded on August 30,2023 at 13:44:49 UTC from IEEE Xplore. Restrictions apply.

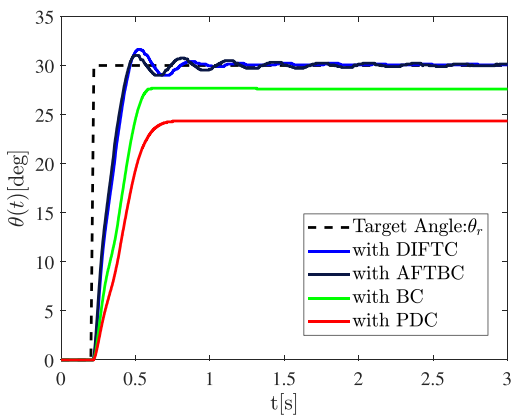

Fig. 8. Angular trajectory with different control methods under 50% partial loss of effectiveness.

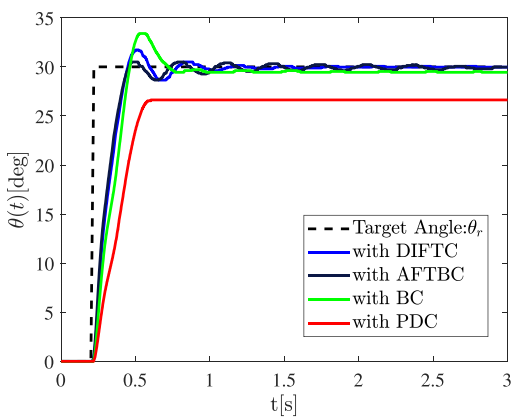

Fig. 9. Angular trajectory with different control methods under 70% partial loss of effectiveness.

The flexible system with actuator faults and an unknown dead-zone cannot reach the desired angle under the BC and PDC, and the tracking error increases as the partial loss of effectiveness increases, implying that the performance is seriously affected. In contrast, the angular tracking can be achieved at 1 s under the AFTBC and DIFTC when meeting different partial losses of effectiveness. Note that, the AFTBC has a larger steady-state error, which can be determined from Table III and the figures. Furthermore, as shown in Fig. 10, the deformation of the link tip can converge to a small neighborhood of zero with DIFTC.

On the basis of the simulation and experimental examples, we conclude that the proposed algorithm can better stabilize the flexible manipulator system with actuator faults and dead-zone nonlinearity with an excellent performance.

VI. Conclusion

To achieve an angle-tracking performance and attenuate the vibration of flexible manipulators with actuator faults and an unknown dead-zone, an adaptive inverse compensation FTC strategy was developed. Smooth dead-zone inverse dynamics were adopted to compensate for dead-zone nonlinearity. An unknown upper-bound adaptive compensation strategy was constructed to offset the effects of compensation errors and actuator bias faults. The uniformly ultimately bounded stability of the controlled system was demonstrated using the Lyapunov's direct method.

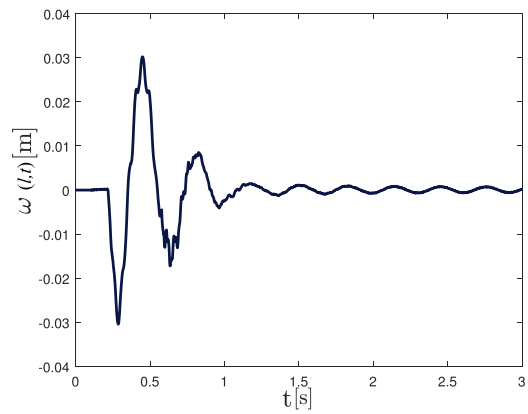

Fig. 10. Boundary deformation with the DIFTC under 70% partial loss of effectiveness.

Simulation and physical experiments were finally performed to verify the efficacy of the DIFTC. The sensor faults [36] and boundary constraints [37], [38], [39] in flexible manipulators will be an interesting topic in a follow-up study.

Appendix A

Lemma 1 [40]: Let $\upsilon_1(z,t)$ and $\upsilon_2(z,t) \in \mathcal{R}$ with $\forall(z,t) \in [0,l] \times [0,+\infty)$ and $\iota > 0$. Then, we derive

$$\upsilon_1\upsilon_2 \le |\upsilon_1\upsilon_2| \le \iota\upsilon_1^2 + \frac{1}{\iota}\upsilon_2^2. \tag{40}$$

Lemma 2 [41]: If there is a variable $\omega(z,t)$ with $\forall(z,t) \in [0,l] \times [0,+\infty)$ satisfying $\omega(0,t) = 0$, we then derive

$$\omega^2 \le l\int_0^l \omega'^2 dz, \qquad \int_0^l \omega^2 dz \le l^2 \int_0^l \omega'^2 dz. \tag{41}$$

Lemma 3 [42]: For any variable χ and positive scalar ζ, the following inequality holds:

$$0 \le |\chi| - \frac{\chi^2}{\sqrt{\chi^2+\zeta^2}} < \zeta \tag{42}$$

if ζ is a positive continuous and bounded function with $\zeta(t)$ satisfying $\lim_{t\to\infty}\int_{t_0}^t \zeta(t)dt \le \bar{\zeta} < \infty$, where $\bar{\zeta}$ is a positive constant, then the abovementioned inequality still holds.

Appendix B

Proof: Invoking Lemmas 1 and 2, we obtain

$$\begin{aligned}|V_{a3}(t)| &\le \eta\rho\int_0^l |\dot{\gamma}\omega|dz + \eta\rho l\int_0^l |\dot{\gamma}[\theta(t)-\theta_r]|dz \\ &\le \frac{\eta\rho(1+l)}{2}\int_0^l \dot{\gamma}^2 dz + \frac{\eta\rho l^2}{2}\int_0^l \omega'^2 dz \\ &\quad + \frac{\eta\rho l^2}{2}[\theta-\theta_r]^2 \le \beta_1(V(t)+V_{a4}(t))\end{aligned} \tag{43}$$

where $\beta_1 = \eta\max\{(1+l), \frac{\rho l^2}{T}, \frac{\rho l^2}{b_\theta}\}$, and

$$V(t) = V_{a1}(t) + V_{a2}(t). \tag{44}$$

Let β_1 satisfy $0 < \beta_1 < 1$, we arrive at

$$0 \le \Lambda_1(V(t)+V_{a4}(t)) \le V_a(t) \le \Lambda_2(V(t)+V_{a4}(t)) \tag{45}$$

with $\Lambda_1 = 1-\beta_1$ and $\Lambda_2 = 1+\beta_1$.

Authorized licensed use limited to: ULAKBIM UASL - Hacettepe Universitesi. Downloaded on August 30,2023 at 13:44:49 UTC from IEEE Xplore. Restrictions apply.

APPENDIX C

Proof: Differentiating (26), we get

$$\dot{V}_a(t) = \dot{V}_{a1}(t) + \dot{V}_{a2}(t) + \dot{V}_{a3}(t) + \dot{V}_{a4}(t). \tag{46}$$

First, integrating by parts and invoking (40) and (41), $\dot{V}_{a1}$ is obtained as

$$\begin{aligned}\dot{V}_{a1}(t) &= \rho\int_0^l \dot{\gamma}\ddot{\gamma}dz + EI\int_0^l \omega''\dot{\omega}''dz + T\int_0^l \omega'\dot{\omega}'dz \\ &= T\int_0^l z\dot{\theta}\omega''dz - c\int_0^l \dot{\gamma}^2dz - EI\omega_0''\dot{\theta} - EIl\dot{\theta}(t)\omega_l''' \\ &\le -EI\omega_0''\dot{\theta}(t) - T\dot{\theta}(t)\omega_l - (c-\phi_1)\int_0^l \dot{\gamma}^2dz \\ &\quad + \frac{1}{\phi_1}\int_0^l f^2dz. \end{aligned}\tag{47}$$

Then, substituting (4) into $\dot{V}_{a2}(t)$, we derive

$$\begin{aligned}\dot{V}_{a2}(t) &= \alpha I\dot{\alpha} + b_\theta[\theta(t)-\theta_r]\dot{\theta}(t) \\ &= \alpha[I\eta\dot{\theta}(t) + T\omega_l + EI\omega_0'' + u(t)] \\ &\quad + b_\theta[\theta(t)-\theta_r]\dot{\theta}(t). \end{aligned}\tag{48}$$

Combining (48) and (19), and using the adaptive controller (20) and (21), we derive

Subsequently, substituting the adaptive laws (22)–(24) into the derivation of function $V_{a4}(t)$ yields

$$\begin{aligned}\dot{V}_{a4}(t) &= -\sigma\tilde{\psi}^T\delta^{-1}\dot{\hat{\psi}} - \frac{\sigma}{\gamma_a}\tilde{p}\dot{\hat{p}} - \tilde{\Theta}\dot{\hat{\Theta}} \\ &= -\sigma\tilde{\psi}^T\delta^{-1}\mathrm{Proj}\{\alpha\delta\hat{\nu}\} - \sigma\alpha\tilde{p}u_d + \frac{\sigma}{\gamma_a}\varrho_2\tilde{p}\hat{p} \\ &\quad - \alpha\tilde{\Theta} + \varrho_1\tilde{\Theta}\hat{\Theta}. \end{aligned}\tag{49}$$

Finally, we obtain the derivative of $V_{a3}(t)$ as

$$\begin{aligned}\dot{V}_{a3}(t) &= \eta\rho\int_0^l \ddot{\gamma}\gamma_d dz + \eta\rho\int_0^l \dot{\gamma}^2dz \\ &= \eta\rho\int_0^l \ddot{\gamma}(\omega + z(\theta(t)-\theta_r))dz + \eta\rho\int_0^l \dot{\gamma}^2dz \\ &= -\eta EI\omega_l\omega_l''' - \eta EI\int_0^l \omega''^2dz + T\eta\omega_l'\omega_l \\ &\quad - T\eta\int_0^l \omega'^2dz - \eta EI[\theta(t)-\theta_r]\omega_0'' \\ &\quad - \eta c\int_0^l \gamma_d\dot{\gamma}dz - T\eta[\theta(t)-\theta_r]\omega_l \\ &\quad + \eta\int_0^l f\gamma_d dz + \eta\rho\int_0^l \dot{\gamma}^2dz. \end{aligned}\tag{50}$$

By combining (47)–(50) into (46), $\dot{V}_a(t)$ is derived as

$$\begin{aligned}\dot{V}_a(t) \le &-\left(c-\phi_1-\eta\rho-\frac{\eta c(1+l)}{2}\right)\int_0^l \dot{\gamma}^2dz \\ &-\left(\eta b_\theta - \eta\phi_4 l^2 - \frac{\eta c l^2}{2}\right)[\theta(t)-\theta_r]^2 \\ &-\left(T\eta - \frac{\eta c l^2}{2} - \eta\phi_3 l^2 - \frac{(b_2+T)l}{2\phi_2}\right)\int_0^l \omega'^2dz \\ &-\left(b_1 - \frac{(b_2+T)\phi_2}{2}\right)\alpha^2 - \eta EI\int_0^l \omega''^2dz \\ &-\frac{\sigma\tilde{\psi}^T\delta^{-1}\tilde{\psi}}{2\lambda_{\max}(\delta^{-1})} - \frac{\sigma}{2\gamma_a}\varrho_2\tilde{p}^2 - \frac{\varrho_1}{2}\tilde{\Theta}^2 + \epsilon \end{aligned}\tag{51}$$

where ϕ_1, ϕ_2, ϕ_3, and $\phi_4 > 0$, and according to the adaptive projection mapping operator, there exists a constant $\psi_m > 0$ satisfying $\|\tilde{\psi}\| \le \psi_m$ and $\epsilon = \zeta(t) + \frac{\sigma}{2\gamma_a}\varrho_2 p^2 + \frac{\varrho_1}{2}\Theta^2 + \frac{\sigma}{2}\psi_m^2 + (\frac{1}{\phi_1} + \frac{\eta}{\phi_3} + \frac{\eta}{\phi_4})l\bar{f}^2 < +\infty$.

Parameters η, b, b_1, b_θ, ϕ_1, ϕ_2, ϕ_3, and ϕ_4 are selected to satisfy the following:

$$\ell_1 = c - \phi_1 - \eta\rho - \frac{\eta c(1+l)}{2} > 0 \tag{52}$$

$$\ell_2 = T\eta - \frac{\eta c l^2}{2} - \eta\phi_3 l^2 - \frac{(b_2+T)l}{2\phi_2} > 0 \tag{53}$$

$$\ell_3 = \eta b_\theta - \eta\phi_4 l^2 - \frac{\eta c l^2}{2} > 0 \tag{54}$$

$$\ell_4 = b_1 - \frac{(b_2+T)\phi_2}{2} > 0. \tag{55}$$

Invoking (52)–(55), we obtain

$$\begin{aligned}\dot{V}_a(t) \le &-\ell_1\int_0^l \dot{\gamma}^2ds - \ell_2\int_0^l \omega'^2ds - \eta EI\int_0^l \omega''^2ds \\ &-\ell_3[\theta(t)-\theta_r]^2 - \ell_4\alpha^2 - \frac{\sigma\tilde{\psi}^T\delta^{-1}\tilde{\psi}}{2\lambda_{\max}(\delta^{-1})} + \epsilon \\ &-\frac{\sigma}{2\gamma_a}\varrho_2\tilde{p}^2 - \frac{\varrho_1}{2}\tilde{\Theta}^2. \end{aligned}\tag{56}$$

Combining (45) and (50) gives

$$\dot{V}_a(t) \le -\Lambda V_a(t) + \epsilon \tag{57}$$

where $\Lambda = \Lambda_3/\Lambda_2$, $\Lambda_3 = \min\{2\ell_1/\rho, 2\eta, 2\ell_2/T, 2\ell_4/I, \varrho_1, 2\ell_3/b_\theta, \varrho_2, 1/\lambda_{\max}(\delta^{-1})\}$.

REFERENCES

[1] Z. Zhao and C. K. Ahn, "Boundary antisaturation vibration control design for a flexible Timoshenko robotic manipulator," *Int. J. Robust Nonlinear Control*, vol. 30, no. 3, pp. 1098–1114, 2020.

[2] B. Niu, C. K. Ahn, H. Li, and M. Liu, "Adaptive control for stochastic switched nonlower triangular nonlinear systems and its application to a one-link manipulator," *IEEE Trans. Syst., Man, Cybern. Syst.*, vol. 48, no. 10, pp. 1701–1714, Oct. 2018.

[3] Z. Zhao, C. K. Ahn, and H.-X. Li, "Boundary antidisturbance control of a spatially nonlinear flexible string system," *IEEE Trans. Ind. Electron.*, vol. 67, no. 6, pp. 4846–4856, Jun. 2020.

[4] X. He, W. He, J. Shi, and C. Sun, "Boundary vibration control of variable length crane systems in two-dimensional space with output constraints," *IEEE/ASME Trans. Mechatronics*, vol. 22, no. 5, pp. 1952–1962, Oct. 2017.

[5] Z. Zhao, Z. Liu, W. He, K.-S. Hong, and H.-X. Li, "Boundary adaptive fault-tolerant control for a flexible timoshenko arm with backlash-like hysteresis," *Automatica*, vol. 130, 2021, Art. no. 109690.

Authorized licensed use limited to: ULAKBIM UASL - Hacettepe Universitesi. Downloaded on August 30,2023 at 13:44:49 UTC from IEEE Xplore. Restrictions apply.

[6] X. He, S. Zhang, Y. Ouyang, and Q. Fu, "Vibration control for a flexible single-link manipulator and its application," *IET Control Theory Appl.*, vol. 14, no. 7, pp. 930–938, 2020.

[7] W. He, X. He, M. Zou, and H. Li, "PDE model-based boundary control design for a flexible robotic manipulator with input backlash," *IEEE Trans. Control Syst. Technol.*, vol. 27, no. 2, pp. 790–797, Mar. 2019.

[8] S. Zhang, R. Liu, K. Peng, and W. He, "Boundary output feedback control for a flexible two-link manipulator system with high-gain observers," *IEEE Trans. Control Syst. Technol.*, vol. 29, no. 2, pp. 835–840, Mar. 2021.

[9] Z. Zhao, X. He, and C. K. Ahn, "Boundary disturbance observer-based control of a vibrating single-link flexible manipulator," *IEEE Trans. Syst., Man, Cybern. Syst.*, vol. 51, no. 4, pp. 2382–2390, Apr. 2021.

[10] Y. Ren, Z. Zhao, C. Zhang, Q. Yang, and K.-S. Hong, "Adaptive neural-network boundary control for a flexible manipulator with input constraints and model uncertainties," *IEEE Trans. Cybern.*, vol. 51, no. 10, pp. 4796–4807, Oct. 2021.

[11] Y. Liu, Y. Wang, Y. Feng, and Y. Wu, "Neural network-based adaptive boundary control of a flexible riser with input deadzone and output constraint," *IEEE Trans. Cybern.*, vol. 52, no. 12, pp. 13120–13128, Dec. 2022.

[12] Z. Zuo, J. Song, W. Wang, and Z. Ding, "Adaptive backstepping control of uncertain sandwich-like nonlinear systems with deadzone nonlinearity," *IEEE Trans. Syst., Man, Cybern. Syst.*, vol. 52, no. 11, pp. 7268–7278, Nov. 2022.

[13] Y.-J. Liu and N. Zhou, "Observer-based adaptive fuzzy-neural control for a class of uncertain nonlinear systems with unknown dead-zone input," *ISA Trans.*, vol. 49, no. 4, pp. 462–469, 2010.

[14] D. Recker, P. Kokotovic, D. Rhode, and J. Winkelman, "Adaptive nonlinear control of systems containing a deadzone," in *Proc. 30th IEEE Conf. Decis. Control*, 1991, pp. 2111–2115.

[15] T. Chen and J. Shan, "Distributed control of multiple flexible manipulators with unknown disturbances and dead-zone input," *IEEE Trans. Ind. Electron.*, vol. 67, no. 11, pp. 9937–9947, Nov. 2020.

[16] J. Zhou, C. Wen, and Y. Zhang, "Adaptive output control of nonlinear systems with uncertain dead-zone nonlinearity," *IEEE Trans. Autom. Control*, vol. 51, no. 3, pp. 504–511, Mar. 2006.

[17] X. Su, Z. Liu, G. Lai, C. L. P. Chen, and C. Chen, "Direct adaptive compensation for actuator failures and dead-zone constraints in tracking control of uncertain nonlinear systems," *Inf. Sci.*, vol. 417, pp. 328–343, 2017.

[18] G. Zhang, M. Yao, W. Zhang, and W. Zhang, "Improved composite adaptive fault-tolerant control for dynamic positioning vehicle subject to the dead-zone nonlinearity," *IET Control Theory Appl.*, vol. 15, no. 16, pp. 2067–2080, 2021.

[19] X. Zhang, T. Parisini, and M. Polycarpou, "Adaptive fault-tolerant control of nonlinear uncertain systems: An information-based diagnostic approach," *IEEE Trans. Autom. Control*, vol. 49, no. 8, pp. 1259–1274, Aug. 2004.

[20] Z. Gao, "Fault estimation and fault-tolerant control for discrete-time dynamic systems," *IEEE Trans. Ind. Electron.*, vol. 62, no. 6, pp. 3874–3884, Jun. 2015.

[21] J.-W. Zhu, C.-Y. Gu, S. X. Ding, W.-A. Zhang, X. Wang, and L. Yu, "A new observer-based cooperative fault-tolerant tracking control method with application to networked multiaxis motion control system," *IEEE Trans. Ind. Electron.*, vol. 68, no. 8, pp. 7422–7432, Aug. 2021.

[22] H. Alwi and C. Edwards, "Fault tolerant control using sliding modes with on-line control allocation," *Automatica*, vol. 44, no. 7, pp. 1859–1866, 2008.

[23] X. Yuan and C. H. T. Lee, "A simple three-degree-of-freedom digital current controller with dead beat response for AC machines," *IEEE Trans. Ind. Electron.*, vol. 69, no. 8, pp. 7848–7858, Aug. 2022.

[24] L. Xing, C. Wen, Z. Liu, H. Su, and J. Cai, "Adaptive compensation for actuator failures with event-triggered input," *Automatica*, vol. 85, pp. 129–136, 2017.

[25] C. Wang, C. Wen, and L. Guo, "Adaptive consensus control for nonlinear multiagent systems with unknown control directions and time-varying actuator faults," *IEEE Trans. Autom. Control*, vol. 66, no. 9, pp. 4222–4229, Sep. 2021.

[26] J. Long, W. Wang, J. Huang, J. Zhou, and K. Liu, "Distributed adaptive control for asymptotically consensus tracking of uncertain nonlinear systems with intermittent actuator faults and directed communication topology," *IEEE Trans. Cybern.*, vol. 51, no. 8, pp. 4050–4061, Aug. 2021.

[27] F. Cao and J. Liu, "Adaptive actuator fault compensation control for a rigid-flexible manipulator with ODEs-PDEs model," *Int. J. Syst. Sci.*, vol. 49, no. 8, pp. 1748–1759, 2018.

[28] X. Zhao, S. Zhang, Z. Liu, and Q. Li, "Vibration control for flexible manipulators with event-triggering mechanism and actuator failures," *IEEE Trans. Cybern.*, vol. 52, no. 8, pp. 7591–7601, Aug. 2022.

[29] Y. Ma, X. He, S. Zhang, Y. Sun, and Q. Fu, "Adaptive compensation for infinite number of actuator faults and time-varying delay of a flexible manipulator system," *IEEE Trans. Ind. Electron.*, vol. 69, no. 12, pp. 13141–13150, Dec. 2022.

[30] Y. Ren, P. Zhu, Z. Zhao, J. Yang, and T. Zou, "Adaptive fault-tolerant boundary control for a flexible string with unknown dead zone and actuator fault," *IEEE Trans. Cybern.*, vol. 52, no. 7, pp. 7084–7093, Jul. 2022.

[31] W. Wang and C. Wen, "Adaptive compensation for infinite number of actuator failures or faults," *Automatica*, vol. 47, no. 10, pp. 2197–2210, 2011.

[32] M. Blanke, M. Kinnaert, J. Lunze, M. Staroswiecki, and J. Schröder, *Diagnosis and Fault-Tolerant Control*. Berlin, Germany: Springer, 2006.

[33] G. Tao and P. V. Kokotovic, *Adaptive Control of Systems With Actuator and Sensor Nonlinearities*. New York, NY, USA: Wiley, 1996.

[34] Z. Liu, J. Liu, and W. He, "Modeling and vibration control of a flexible aerial refueling hose with variable lengths and input constraint," *Automatica*, vol. 77, pp. 302–310, 2017.

[35] M. Krstic, I. Kanellakopoulos, and P. V. Kokotovic, *Nonlinear and Adaptive Control Design*. New York, NY, USA: Wiley, 1995.

[36] D. Ye, Y. Xiao, Z. Sun, and B. Xiao, "Neural network based finite-time attitude tracking control of spacecraft with angular velocity sensor failures and actuator saturation," *IEEE Trans. Ind. Electron.*, vol. 69, no. 4, pp. 4129–4136, Apr. 2022.

[37] S. He, L. Kou, Y. Li, and J. Xiang, "Position tracking control of fully-actuated underwater vehicles with constrained attitude and velocities," *IEEE Trans. Ind. Electron.*, vol. 69, no. 12, pp. 13192–13202, Dec. 2022.

[38] Y. Cao, C. Wen, and Y. Song, "A unified event-triggered control approach for uncertain pure-feedback systems with or without state constraints," *IEEE Trans. Cybern.*, vol. 51, no. 3, pp. 1262–1271, Mar. 2021.

[39] J. Huang, W. Wang, and J. Zhou, "Adaptive control design for underactuated cranes with guaranteed transient performance: Theoretical design and experimental verification," *IEEE Trans. Ind. Electron.*, vol. 69, no. 3, pp. 2822–2832, Mar. 2022.

[40] Z. Liu, Z. Han, Z. Zhao, and W. He, "Modeling and adaptive control for a spatial flexible spacecraft with unknown actuator failures," *Sci. China Inf. Sci.*, vol. 64, 2021, Art. no. 152208.

[41] G. H. Hardy et al., *Inequalities*. Cambridge, U.K.: Cambridge Univ. Press, 1952.

[42] Y.-X. Li and G.-H. Yang, "Adaptive asymptotic tracking control of uncertain nonlinear systems with input quantization and actuator faults," *Automatica*, vol. 72, pp. 177–185, 2016.

Zhijia Zhao (Member, IEEE) received the B.Eng. degree in automatic control from the North China University of Water Resources and Electric Power, Zhengzhou, China, in 2010, and the M.Eng. and Ph.D. degrees in automatic control from the South China University of Technology, Guangzhou, China, in 2013 and 2017, respectively.

He is currently an Associate Professor with the School of Mechanical and Electrical Engineering, Guangzhou University, Guangzhou. His research interests include adaptive and learning control, flexible mechanical systems, and robotics.

Zhifeng Tan received the B.Eng. degree in robotics engineering in 2021 from Guangzhou University, Guangzhou, China, where he is currently working toward the master's degree in automatic control.

His research interests include flexible systems, distributed parameter system control, robotics, and adaptive control.

Authorized licensed use limited to: ULAKBIM UASL - Hacettepe Universitesi. Downloaded on August 30,2023 at 13:44:49 UTC from IEEE Xplore. Restrictions apply.

Zhijie Liu (Member, IEEE) received the B.Sc. degree from the China University of Mining and Technology Beijing, Beijing, China, in 2014 and the Ph.D. degree from Beihang University, Beijing, China, in 2019, both in automatic control.

In 2017, he was a Research Assistant with the Department of Electrical Engineering, University of Notre Dame, Notre Dame, IN, USA, for 12 months. He is currently a Professor with the School of Intelligence Science and Technology, University of Science and Technology Beijing, Beijing. His research interests include adaptive control, modeling and vibration control for flexible structures, and distributed parameter systems.

Mehmet Onder Efe (Senior Member, IEEE) received the B.Sc. degree in electronics and communications engineering from Istanbul Technical University, Istanbul, Turkey, in 1993, the M.Sc. degree in systems and control engineering from Boğazici University, Istanbul, in 1996, and the Ph.D. degree in electrical and electronics engineering from Boğazici University, in 2000.

He is currently a Professor with the Department of Computer Engineering, Hacettepe University, Ankara, Turkey.

Dr. Efe serves and served as an Associate Editor for the IEEE Transactions on Industrial Electronics, IEEE Transactions on Industrial Informatics, IEEE/ASME Transactions on Mechatronics, and Editor for *Transactions of the Institute of Measurement* and *Control and Measurement and Control*.

Choon Ki Ahn (Senior Member, IEEE) received the B.S. and M.S. degrees from the School of Electrical Engineering, Korea University, Seoul, South Korea, in 2000 and 2002, respectively, and the Ph.D. degree from the School of Electrical Engineering and Computer Science, Seoul National University, Seoul, South Korea, in 2006, all in electrical engineering.

He is currently a Crimson Professor of Excellence with the College of Engineering and a Full Professor with the School of Electrical Engineering, Korea University.

Dr. Ahn was the recipient of the Early Career Research Award of Korea University in 2015. In 2016, he was ranked #1 in Electrical/Electronic Engineering among Korean young professors based on research quality, the *Presidential Young Scientist Award* from the President of South Korea, in 2017, the Outstanding Associate Editor Award for IEEE Transactions on Neural Networks and Learning Systems, in 2020, Best Associate Editor Award for *IEEE Transactions on Systems, Man, and Cybernetics: Systems*, in 2021. In 2019–2022, he was also the recipient of Research Excellence Award from Korea University (Top 3% Professor of Korea University in Research). He has been a Senior Editor for IEEE Transactions on Neural Networks and Learning Systems, a Senior Associate Editor for IEEE Systems Journal, and an Associate Editor for IEEE Transactions on Fuzzy Systems, IEEE Transactions on Systems, Man, and Cybernetics: Systems, IEEE Transactions on Automation Science and Engineering, IEEE Transactions on Intelligent Transportation Systems, IEEE Transactions on Circuits and Systems I: Regular Papers, IEEE Systems, Man, and Cybernetics Magazine, *Nonlinear Dynamics, Aerospace Science and Technology*, and*other flagship journals*. He is the recipient of the 2019–2022 Highly Cited Researcher Award in Engineering by Clarivate Analytics (formerly, Thomson Reuters).

Authorized licensed use limited to: ULAKBIM UASL - Hacettepe Universitesi. Downloaded on August 30,2023 at 13:44:49 UTC from IEEE Xplore. Restrictions apply.